ELSEVIER

Journal of Nuclear Materials 250 (1997) 83–87

journal of nuclear materials

Melting behaviour of oxide systems for heterogeneous transmutation of actinides.
II. The system $MgO–Al_2O_3–PuO_2$

Hengzhong Zhang [1], M.E. Huntelaar, R.J.M. Konings *, E.H.P. Cordfunke

Netherlands Energy Research Foundation ECN, P.O.Box 1, 1755 ZG Petten, The Netherlands

Received 16 June 1997; accepted 18 September 1997

Abstract

Isothermal sections of the phase diagram of the system $MgO–Al_2O_3–PuO_2$ at various temperatures were calculated using sublattice models. The results show that below 2133 K no liquid occurs in the system. Above 2133 K liquid starts to form at the $Al_2O_3–PuO_2$ side. The phase diagram of the pseudo-binary system $PuO_2–MgAl_2O_4$ was also obtained from an isopleth $T–x$ calculation. © 1997 Elsevier Science B.V.

1. Introduction

Experiments show that magnesium aluminate spinel ($MgAl_2O_4$) is more resistant toward neutron irradiation than several other oxide matrix candidates for heterogeneous transmutation of actinides such as Al_2O_3, MgO and $Y_3Al_5O_2$ [1]. The thermal diffusivity of single-crystal spinel hardly changes after neutron irradiation, while those of MgO and Al_2O_3 change drastically. Even in polycrystals, the thermal diffusivity of spinel changes much less than those of MgO and Al_2O_3. The swelling of spinel after neutron irradiation is also less [2], and its resistance to cooling media of reactors (water, liquid sodium) is good [1,3]. Therefore, spinel is a very promising matrix material for heterogeneous transmutation of plutonium.

Nevertheless, the melting behaviour of the system comprised by $MgAl_2O_4$ and PuO_2 remains unknown, basically because experiments are difficult due to the very high radiotoxicity of plutonium compounds and the necessity of very high temperatures. Yet, the melting behaviour of the system is essential to evaluate the properties of spinel-based fuels for heterogeneous transmutation of plutonium. In the present work the melting behaviour of the system $PuO_2–MgAl_2O_4$ was therefore studied by phase diagram calculations of the ternary system $MgO–Al_2O_3–PuO_2$.

2. Literature review

There are three binary boundary systems in the ternary system $MgO–Al_2O_3–PuO_2$: $MgO–PuO_2$, $Al_2O_3–PuO_2$ and $MgO–Al_2O_3$. Experimental information about the phase equilibria in the former two binary systems is very scarce. In the authors' previous work [4], the phase diagrams of the systems $MgO–PuO_2$ and $Al_2O_3–PuO_2$ were optimized with the association model and the Redlich–Kister (R–K) method, based on the limited experimental information available in Ref. [5].

To the contrary, extensive experimental information about the phase equilibria of the system $MgO–Al_2O_3$ can be found (Ref. [6]). Nevertheless, the understanding of the phase relations in this system is often difficult because of the inconsistencies in the experimental data. Several thermodynamic assessments were made for this system. Kaufman et al. [7] treated $MgAl_2O_4$ as a stoichiometric compound, and modelled the liquid phase with a simple R–K

---

* Corresponding author. Tel.: +31-224 564 138; fax: +31-224 563 608; e-mail: konings@ecn.nl.

[1] Visiting scientist on leave from Department of Chemistry, Central South University of Technology, Changsha, Hunan 410083, People's Republic of China.

PII S0022-3115(97)00289-4

method. This treatment seems too simple because it neglects the non-stoichiometry of $MgAl_2O_4$. Howald et al. [8,9] used a sublattice model to treat the spinel phase, and a simple R–K equation to model the liquid phase. An unusual steep increase in the liquidus of spinel can be observed in their calculated diagram. Eriksson et al. [10] used modified quasi-chemical models for the liquid phase as well as the $MgAl_2O_4$ phase, but no deviation from the stoichiometric composition on the MgO side was taken into account. Another assessment of the system was made by Hallstedt [6]. In this work the compound energy model was used to describe the spinel phase and a two-sublattice model was used to describe the liquid phase. Both the hypo- and the hyperstoichiometry of spinel were taken into account.

By comparing the thermodynamic treatments employed and the phase diagrams calculated in the above Refs. [6–10], it is clear that the work of Hallstedt [6] is the most reliable one. Therefore, in our present work we will make use of the thermodynamic description of the system MgO–Al_2O_3 in Ref. [6] and combine it with our re-modelling of the MgO–PuO_2 and Al_2O_3–PuO_2 systems [4] to carry out the phase diagram calculation of the ternary system MgO–Al_2O_3–PuO_2.

3. Method of calculation

In the present work, the programs PARROT and POLY-3 included in Thermo-Calc [11] have been used to perform the phase diagram optimization and phase diagram calculation. Because the liquid phase in the MgO–Al_2O_3 system was already modelled using a two-sublattice model in Ref. [6], the phase diagrams of the two boundary systems MgO–PuO_2 and Al_2O_3–PuO_2 assessed in our previous work [4] have been re-optimized using sublattice models to describe the liquid phase of the ternary system MgO–Al_2O_3–PuO_2 consistently. In the calculation, thermodynamic data of pure oxides are taken from ECN-Tbase [12] and SGTE [6].

4. Phase diagram calculations

4.1. Binary systems

4.1.1. MgO–PuO_2

The three phases present in the MgO–PuO_2 system are modelled by the following sublattice models in accordance with the literature [6]:

halite phase: $(Mg^{2+})_1(O^{2-})_1$
fcc phase: $(Mg^{2+}, Pu^{4+}, Va)_2(O^{2-})_2$
liquid phase: $(Mg^{2+}, Pu^{4+})_2(O^{2-})_q$,

where Va represents a vacancy in the fcc phase. For simplicity, in subsequent descriptions we will use M, O, P and V to denote Mg^{2+}, O^{2-}, Pu^{4+} and Va, respectively, and use y to denote their site fractions in a sublattice. Subscript q denotes the anion site number in the liquid phase, it is variable in order to make electroneutrality: $q = 2y_M + 4y_P$. In terms of the sublattice-model formalization [6,13], the Gibbs energies of these phases are

$$G(\text{halite}) = G^0(\text{MgO(halite)}), \tag{1}$$

$$\begin{aligned} G(\text{fcc}) &= y_M G^0_{M_2O_2} + y_P G^0_{P_2O_2} + y_V G^0_{V_2O_2} \\ &\quad + 2RT(y_M \ln y_M + y_P \ln y_P + y_V \ln y_V) \\ &\quad + G^E(\text{fcc}), \end{aligned} \tag{2}$$

$$\begin{aligned} G(\text{liquid}) &= 2y_M G^0(\text{MgO(liquid)}) \\ &\quad + 2y_P G^0(\text{PuO}_2(\text{liquid})) \\ &\quad + 2RT(y_M \ln y_M + y_P \ln y_P) + G^E(\text{liquid}). \end{aligned} \tag{3}$$

In Eq. (2), the contributions to G^E(fcc) of the interactions between Mg^{2+} and Va, Pu^{4+} and Va in the fcc cation sublattice can be set to zero as suggested in Ref. [6]; a sub-regular solution model is used to describe the contribution from the interaction between Mg^{2+} and Pu^{4+}:

$$G^E = y_M y_P [A + B(y_M - y_P)] \tag{4}$$

$G^0_{M_2O_2} = 2G^0(\text{MgO(fcc)})$; $G^0_{V_2O_2} = G^0(\text{Va}_2(\text{O}^{2-})_2) = 0$ in accordance with Ref. [6]; $G^0_{P_2O_2} = G^0((\text{Pu}^{4+})_2(O^2-)_2)$. $G^0_{P_2O_2}$ can be deduced from Eq. (2) when $y_M = 0$, $y_P = 0.5$ and $y_V = 0.5$. In this case the fcc phase becomes pure PuO_2:

$$\begin{aligned} G^0(\text{PuO}_2(\text{fcc})) &= 0.5\left[G^0_{P_2O_2} + G^0_{V_2O_2}\right] \\ &\quad + 2RT(0.5\ln 0.5 + 0.5\ln 0.5) + 0 \\ &= 0.5\left(G^0_{P_2O_2} + G^0_{V_2O_2} - 4RT\ln 2\right) \\ &= 0.5\left(G^0_{P_2O_2} - 4RT\ln 2\right). \end{aligned} \tag{5}$$

Thus,

$$G^0_{P_2O_2} = 2G^0(\text{PuO}_2(\text{fcc})) + 4RT\ln 2. \tag{6}$$

In Eq. (3), the excess Gibbs energy of the liquid phase can also be described by a sub-regular solution equation; its form is the same as Eq. (4).

Based on the phase diagram of the MgO–PuO_2 system given in Ref. [4], the sublattice model parameters in the present description can be optimized (Ref. [14]). The re-optimized phase diagram obtained in this way agrees reasonably well with that obtained by the association model in Ref. [4].

4.1.2. Al_2O_3–PuO_2

The three phases present in the Al_2O_3–PuO_2 system can be modelled with the following sublattice models in accordance with the literature [6]:

hex (hexagonal) phase: $(Al^{3+})_2(O^{2-})_3$
fcc phase: $(Pu^{4+}, Va)_2(O^{2-})_2$
liquid phase: $(Al^{3+}, Pu^{4+})_2(O^{2-})_q$

The Gibbs energies of these phases can be represented by

$$G(\text{hex}) = G^0(\text{Al}_2\text{O}_3(\text{hex})), \tag{7}$$

$$G(\text{fcc}) = y_\text{P} G^0_{\text{P}_2\text{O}_2} + y_\text{V} G^0_{\text{V}_2\text{O}_2} + 2RT(y_\text{P} \ln y_\text{P} + y_\text{V} \ln y_\text{V}) + G^E(\text{fcc}), \tag{8}$$

$$G(\text{liquid}) = y_\text{A} G^0(\text{Al}_2\text{O}_3(\text{liquid})) + 2 y_\text{P} G^0(\text{PuO}_2(\text{liquid})) + 2RT(y_\text{A} \ln y_\text{A} + y_\text{P} \ln y_\text{P}) + G^E(\text{liquid}), \tag{9}$$

where A denotes Al^{3+} in a cation sublattice.

In fact the fcc phase in this system is a special case of that in the MgO–PuO_2 system when $y_M = 0$. The meanings of the symbols in Eq. (8) are the same as those in Eq. (2). As a result, the G^E term in Eq. (8) is equal to zero. Eq. (9) is similar to Eq. (3), the difference lies in the fact that the excess energy is a result of the interaction between Al^{3+} and Pu^{4+} instead of Mg^{2+} and Pu^{4+}.

In the Al_2O_3–PuO_2 system, the only experimental information available is a eutectic point from Ref. [5]. Based on the experimental data the sublattice model parameters were optimized (Ref. [14]). The calculated phase diagram obtained in this way agrees reasonably well with that obtained by the association model in Ref. [4].

4.1.3. MgO–Al_2O_3

The four phases present in the MgO–Al_2O_3 system were described as follows in the literature [6]:

hex phase: $(Al^{3+})_2(O^{2-})_3$
halite phase: $(Mg^{2+}, Al^{3+}, Va)_1(O^{2-})_1$
spinel phase: $(Al^{3+}, Mg^{2+})_1(Al^{3+}, Mg^{2+}, Va)_2(Mg^{2+}, Va)_2(O^{2-})_4$
liquid phase: $(Al^{3+}, Mg^{2+})_2(O^{2-})_q$

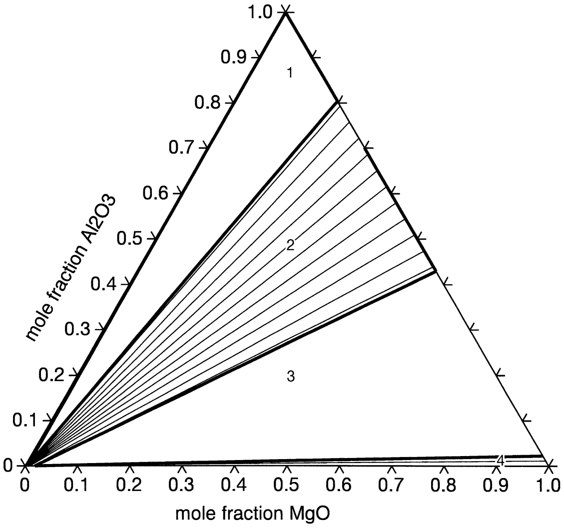

Fig. 1. Calculated phase diagram of the system MgO–Al_2O_3–PuO_2 at 2100 K; (1) fcc + hex + spinel; (2) fcc + spinel; (3) fcc + halite + spinel; (4) fcc + halite.

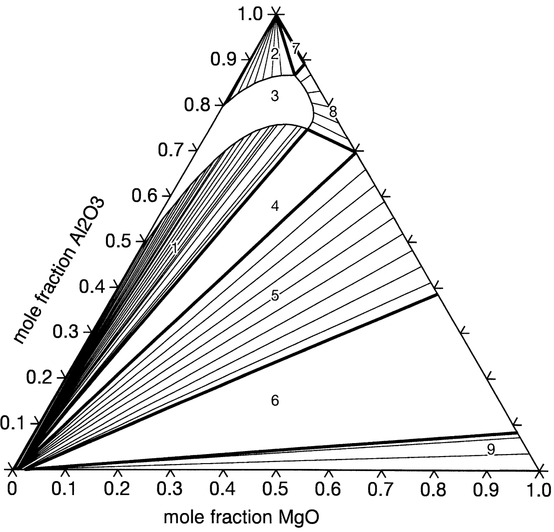

Fig. 2. Calculated phase diagram of the system MgO–Al_2O_3–PuO_2 at 2250 K. (1) fcc + L; (2) hex + L; (3) L; (4) L + spinel + fcc; (5) fcc + spinel; (6) fcc + spinel + halite; (7) spinel + L + hex; (8) spinel + L; (9) fcc + halite.

The model parameters which were obtained by optimization by Hallstedt [6], were used in the present calculations.

4.2. The MgO–Al_2O_3–PuO_2 system

To be consistent with the sublattice descriptions of the phases present in the three binary systems MgO–PuO_2,

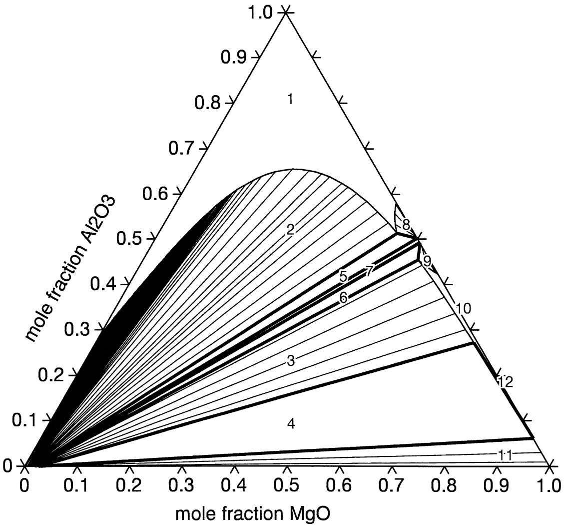

Fig. 3. Calculated phase diagram of the system MgO–Al_2O_3–PuO_2 at 2360 K. (1) L; (2) fcc + L; (3) fcc + L; (4) fcc + L + halite; (5) fcc + L + spinel; (6) fcc + L + spinel; (7) fcc + spinel; (8) spinel + L; (9) spinel + L; (10) L; (11) fcc + halite; (12) halite + L.

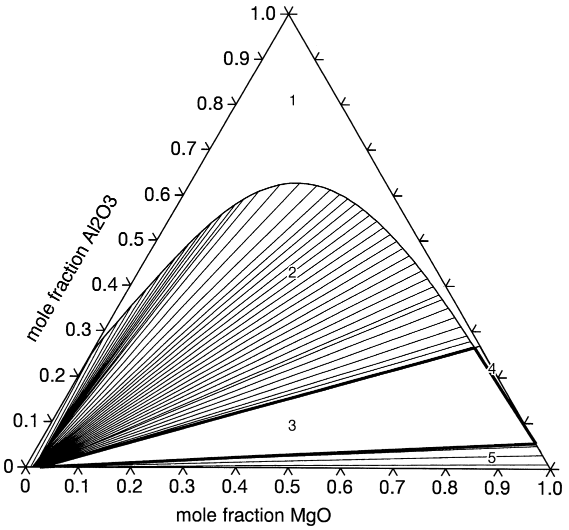

Fig. 4. Calculated phase diagram of the system MgO–Al_2O_3–PuO_2 at 2380 K. (1) L; (2) fcc + L; (3) fcc + L + halite; (4) halite + L; (5) fcc + halite.

Al_2O_3–PuO_2 and MgO–Al_2O_3, the five phases present in the ternary system MgO–Al_2O_3–PuO_2 can be described by the following sublattice models:

hex phase: $(Al^{3+})_2(O^{2-})_3$
halite phase: $(Mg^{2+}, Al^{3+}, Va)_1(O^{2-})_1$
fcc phase: $(Mg^{2+}, Pu^{4+}, Va)_2(O^{2-})_2$
spinel phase: $(Al^{3+}, Mg^{2+})_1(Al^{3+}, Mg^{2+}, Va)_2(Mg^{2+}, Va)_2(O^{2-})_4$
liquid phase: $(Al^{3+}, Mg^{2+}, Pu^{4+})_2\ (O^{2-})_q$.

In the spinel phase, Pu^{4+} is not considered as a constituent of a sublattice because PuO_2 has a CaF_2 structure which is different from the spinel ($MgAl_2O_4$) structure.

All the interaction parameters between species in a sublattice of one phase are from the three binary systems (Refs. [6,14]). The Muggianu method [15] is used to predict the behaviour of a ternary system from its boundary binaries. No ternary interaction term is used here because of lack of experimental information on the ternary system MgO–Al_2O_3–PuO_2. Figs. 1–4 show the calculated isothermal sections of the ternary system MgO–Al_2O_3–PuO_2 at selected temperatures.

It can be seen from Figs. 1–4 that

- At 2100 K, no liquid is present.
- At 2250 K, liquid starts to form at the Al_2O_3–PuO_2 side.
- At 2360 K, 12 phase fields, including two liquid fields, are present in the system. The phase relations at this temperature are very complex, because there are many phase transformations in the MgO–Al_2O_3 boundary system.
- At 2380 K, the two liquid fields in Fig. 3 are merged.

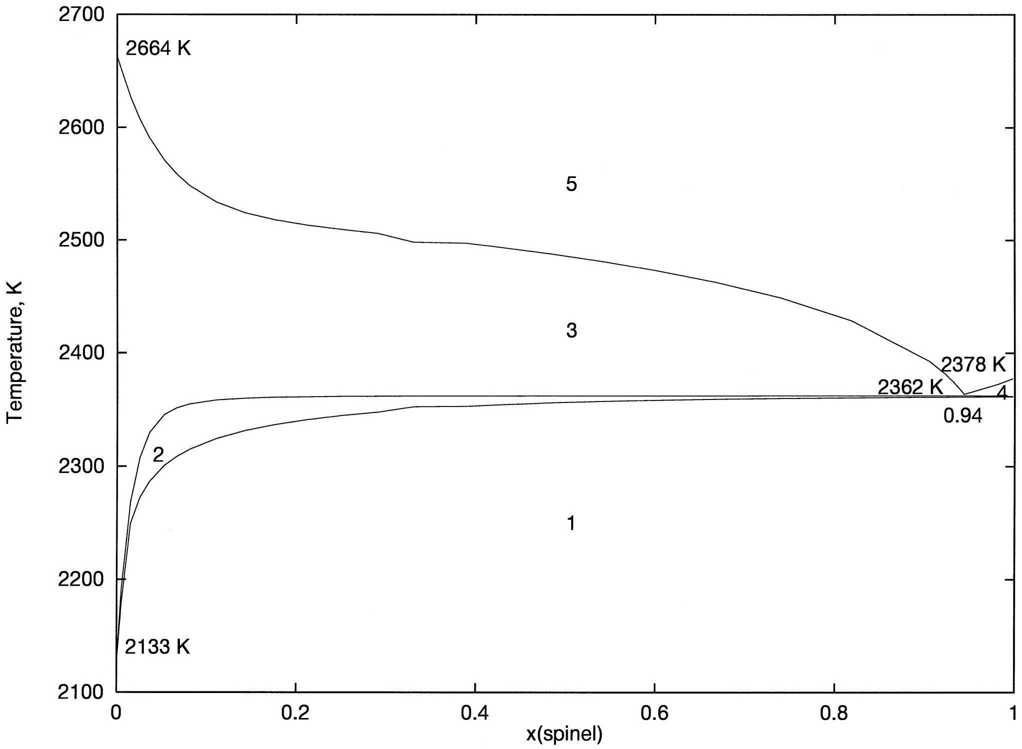

Fig. 5. Calculated phase diagram of the pseudo-binary system PuO_2–spinel. (1) fcc + spinel; (2) fcc + spinel + L; (3) L + fcc; (4) L + spinel; 5, L

4.3. The pseudo-binary system PuO_2–$MgAl_2O_4$

A special section in the ternary system MgO–Al_2O_3–PuO_2 is the isopleth *T*–*x* section starting from PuO_2 to $MgAl_2O_4$ (spinel). This system is of great importance to the heterogeneous transmutation of plutonium when using spinel as the matrix material. Fig. 5 shows the calculated phase diagram of this pseudo-binary system. It can be seen from the figure that the solidus of fcc + spinel + L is not a straight line, especially on the PuO_2 side. Because the fcc phase is a solid solution and the spinel phase is a non-stoichiometric compound, they do not have definite compositions, thus the actual equilibrium tie line between the fcc phase and the spinel phase may significantly deviate from the connection line between PuO_2 and $MgAl_2O_4$ (see Fig. 2), though the overall system composition is on the connection line. This accounts for a remarkable decrease of the solidus temperature of fcc + spinel + L phases on the PuO_2 side. The same reason accounts for the shape of the curve between fcc + spinel + L and L + fcc. Combining Fig. 5 with Figs. 1 and 2, it is evident that the temperature 2133 K is the lowest temperature at which liquid occurs in the ternary system MgO–Al_2O_3–PuO_2.

5. Discussion and conclusion

According to Fig. 5, a nuclear fuel composed of $PuO_2 + MgAl_2O_4$ exists of two separate phases at low temperatures, the fcc phase and the spinel phase. When the temperature increases, a liquid is formed. This temperature, which is referred to as the ‘melting temperature’: of the mixture, can be predicted by the solidus temperature of the fcc + spinel + L phases. Eq. (10) is the regression representation of the ‘melting temperature’:

$$T_m = 2133 + 13516x/(1 + 60.5x - 2.8x^2), \tag{10}$$

where x is the mole fraction of spinel in the mixture PuO_2 + spinel.

The concentration of PuO_2 in a heterogeneous inert-matrix fuel can range from a few % up to 40% by volume. In this composition range the ‘melting temperature’ is close to the eutectic temperature, 2362 K. However, local melting of a $PuO_2 + MgAl_2O_4$ fuel may occur in case of an inhomogeneous distribution of PuO_2 over the pellets, since there is a steep decrease in the ‘melting temperature’ on the PuO_2 side. In order to avoid local melting phenomena, a homogeneous dispersion of fine-grained PuO_2 particles in the target is therefore to be preferred from the point of view of the present analysis. This should, however, be matched with criteria for thermal conductivity and mechanical properties [16].

References

[1] C. Prunier, Y. Guerin, J. Faugere, N. Cocuaud, J. M. Adnet, Proceedings GLOBAL’95, International Conference on Evaluation of Emerging Nuclear Fuel Cycle Systems, Versailles, France, Sept. 11–14, 1995, p. 506.
[2] R.J.M. Konings, K. Bakker, J.G. Boshoven, R. Conrad, H. Hein, J. Nucl. Mater., submitted.
[3] R.J.M. Konings, K. Bakker, J.G. Boshoven, H. Hein, M.E. Huntelaar, J.D. Meeldijk, C.F. Woensdregt, H. Zhang, Proceedings GLOBAL’97, International Conference on Future Nuclear, Yokohama, Japan, Oct. 6–10, 1997, p. 670.
[4] H. Zhang, M.E. Huntelaar, R.J.M. Konings, E.H.P. Cordfunke, J. Nucl. Mater. 249 (1997) 223.
[5] A. Hough, J.A.C. Marples, J. Nucl. Mater. 15 (1965) 298.
[6] B. Hallstedt, J. Am. Ceram. Soc. 75 (1992) 1497.
[7] L. Kaufman, H. Nesor, Calphad 2 (1978) 35.
[8] R.A. Howald, B.N. Roy, Calphad 15 (1991) 159.
[9] R.A. Howald, Calphad 18 (1994) 21.
[10] G. Eriksson, P. Wu, A.D. Pelton, Calphad 17 (1993) 189.
[11] B. Sundman, Thermo-Calc User’s Guide, Royal Institute of Technology, Sweden, 1995.
[12] E.H.P. Cordfunke, R.J.M. Konings, J. Phase Equilib. 14 (1993) 457.
[13] M. Hillert, B. Jansson, B. Sundman, J. Agren, Metall. Trans. 16A (1985) 261.
[14] H. Zhang, M.E. Huntelaar, R.J.M. Konings, E.H.P. Cordfunke, Melting behaviour of oxide systems for heterogeneous transmutation of actinides, Netherlands Energy Research Foundation ECN, Report ECN-I-96-050, 1996.
[15] M. Hillert, Calphad 4 (1980) 1.
[16] K. Bakker, R.J.M. Konings, J. Alloys Comp., in press.